ELSEVIER

Applied Catalysis A: General 154 (1997) 139–153

APPLIED CATALYSIS A: GENERAL

The influence of reaction temperature on the cracking mechanism of *n*-hexane over H-ZSM-48

D. Bhattacharya, S.S. Tambe, S. Sivasanker*

National Chemical Laboratory, Pune-411008, India

Received 29 May 1996; received in revised form 13 December 1996; accepted 20 December 1996

Abstract

The cracking of *n*-hexane at different temperatures over H-ZSM-48 has been analyzed using an established kinetic model. The model includes a monomolecular cracking path based on Langmuir adsorption isotherm as well as a bimolecular path following Rideal kinetics which accounts for the possibility of a chain mechanism being involved. Catalyst decay is accounted by using a time on stream decay function. The scrutiny of the optimal parameters for the model describing *n*-hexane conversion suggests that the catalyst surface composition is sensitive to temperature owing to the difference in the enthalpy of adsorption between the reactant and the average product of the cracking. As the temperature increases, the reactant competes more successfully for the active sites. The average activation energy for protolytic cracking of *n*-hexane on H-ZSM-48 was found to be 20.2 kcal mol^{-1}. Steric inhibition during hydrogen transfer between *n*-hexane and C_4 and C_3 olefins is also observed.

Keywords: *n*-hexane; H-ZSM-48; Cracking mechanism; Protolytic cracking; Chain mechanism in cracking

1. Introduction

Fluid Catalytic Cracking (FCC) is the primary refinery process for producing gasoline. Cracking of paraffins has also been used for the characterization of the catalytic activities and pore dimensions of zeolites by the 'α-test' (cracking of *n*-hexane) [1–4] and the constraint index (relative cracking of *n*-hexane and 3-methyl pentane) [5]. This has generated an associated interest in the kinetic analysis of FCC processes. Recently, kinetic and mechanistic studies of the reaction of C_6 paraffins carried out on HY and other large-pore zeolites have indicated that the cracking of these molecules follows both protolytic and chain reaction modes

* Corresponding author.

0926-860X/97/$17.00 © 1997 Elsevier Science B.V. All rights reserved.
PII S0926-860X(97)00008-2

[6–9]. Optimum values of the kinetic parameters obtained from fitting experimental conversion data as a function of contact time showed that the relative importance of these reaction modes depends on the properties of the catalyst and the reaction temperature. Most of the kinetic studies on the cracking of C_6-paraffins have been conducted over zeolites such as HY and USHY (which are components of FCC catalysts) and no detailed kinetic study of paraffin cracking is available over the medium pore zeolite, H-ZSM-48. It is already known that the paraffin cracking network over HY or USHY is influenced by the framework and extra framework aluminium [10] and dilution of the feed with inert gas like N_2 [11]. Hydride transfer from the feed molecule to a lower carbenium ion that proceeds through a bimolecular transition state, is one of the important steps during paraffin cracking. It has been found that the hydrogenation activity of C_3 and C_4 olefins depends on the pore structure of the zeolite [12]. Abbot et al. [13] have studied cracking reaction over large-pore zeolites and showed that in all linear alkane cracking reactions, the kinetic equation does not require the term accounting for the chain process. In this context, it is important to examine the occurrence of a chain process during paraffin cracking over medium pore zeolites, taking H-ZSM-48 as a model medium pore zeolite.

In this paper, we assume that *n*-hexane cracking over H-ZSM-48 proceeds via both the mechanisms viz., the monomolecular protolytic cracking and the biomolecular chain mechanism. Conversion of *n*-hexane is plotted against contact time at different reaction times and the nonlinear conversion vs. contact time plots at specific temperature are used to estimate the optimal kinetic parameters. The analysis of the estimated kinetic parameters has indicated the possibility of the chain mechanism in the cracking network. The average activation energy for the protolytic process and the difference in the enthalpy of adsorption between the reactant and the average product were computed. Additionally the reactivity of the C_2–C_4 olefins in the hydrogen transfer step and their dependencies on the zeolite pore structure have been examined.

1.1. Theory

This kinetic study is based on the instantaneous fraction conversion and selectivity data. The methodology for determining the initial selectivity of products from the experimental product yield and conversion data has been defined by Ko et al. [14]. For each reaction, the yield of the product is plotted against the conversion. Each of the plots is enveloped by a single curve known as the optimum performance envelop (OPE), that describes the selectivity behavior of a product as the catalyst decay approaches to zero. Figs. 1–3 show some of the OPE plots obtained in *n*-hexane cracking at 420, 450 and 500°C. The initial weight selectivities of the products estimated from the initial slope of the conversion vs. product yield of the product are presented in Table 1. Initial molar selectivities (Table 2) were calculated from the initial weight selectivities that are listed in Table 1 using

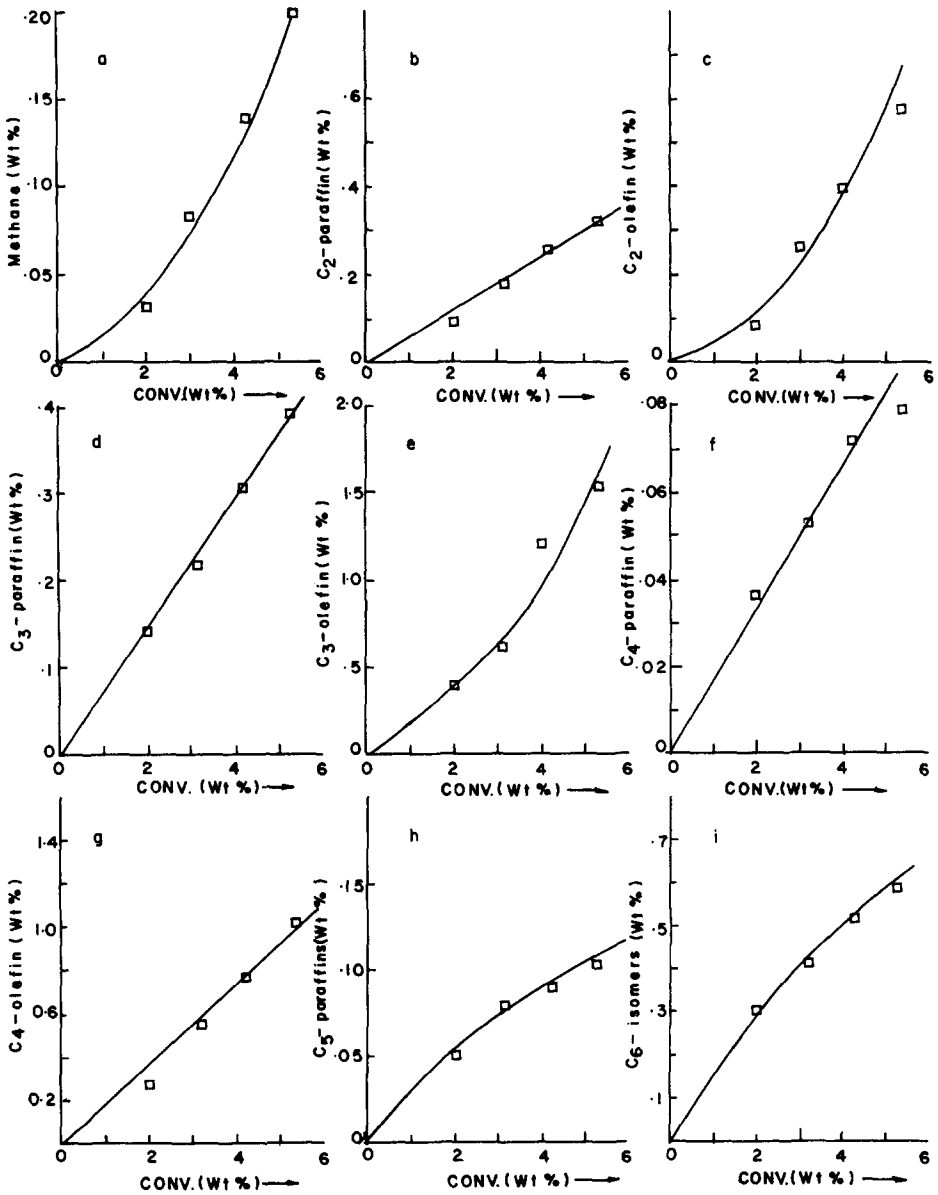

Fig. 1. Optimum performance envelopes for the products of the reaction of *n*-hexane over H-ZSM-48 at 420°C: (a) Methane; (b) C_2-paraffin C_2-olefin; (d) C_3-paraffin; (e) C_3-olefin; (f) C_4-paraffins; (g) C_4-olefins; (h) C_5-paraffins; (i) C_6-isomers.

the relationship:

$$\text{molar selectivity} = \text{weight selectivity} \times \frac{\text{molecular weight of the feed}}{\text{molecular weight of product}}.$$

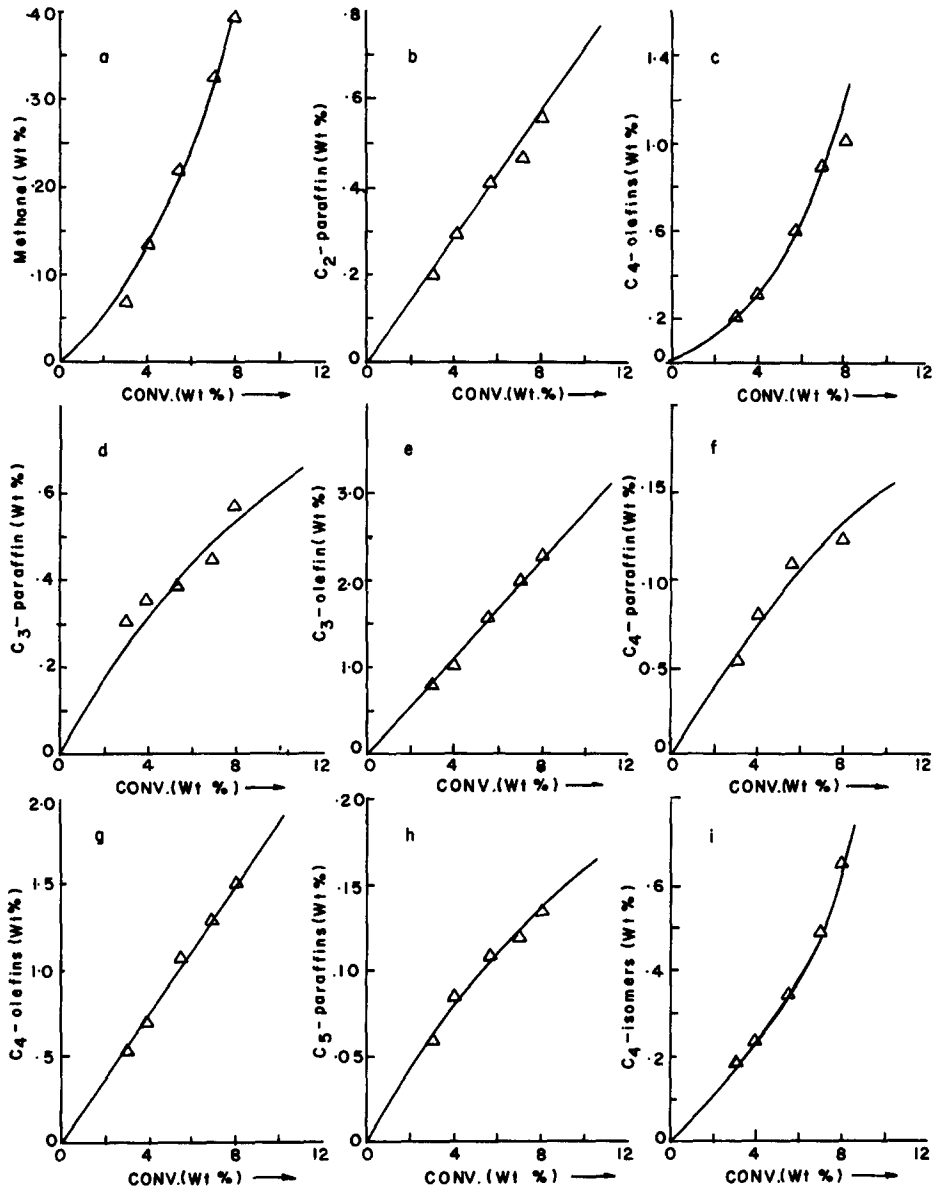

Fig. 2. Optimum performance envelopes for the products of the reaction of *n*-hexane over H-ZSM-48 at 450°C: (a) Methane; (b) C_2-paraffin C_2-olefin; (d) C_3-paraffin; (e) C_3-olefin; (f) C_4-paraffins; (g) C_4-olefins; (h) C_5-paraffins; (i) C_6-isomers.

The kinetic model used in this study was proposed by Groten et al. [15]. The model accounts for the monomolecular protolysis and the bimolecular chain processes. It assumes that the same sites catalyzed both the mechanisms and the surface reaction is the rate controlling step. Solution of the model equation

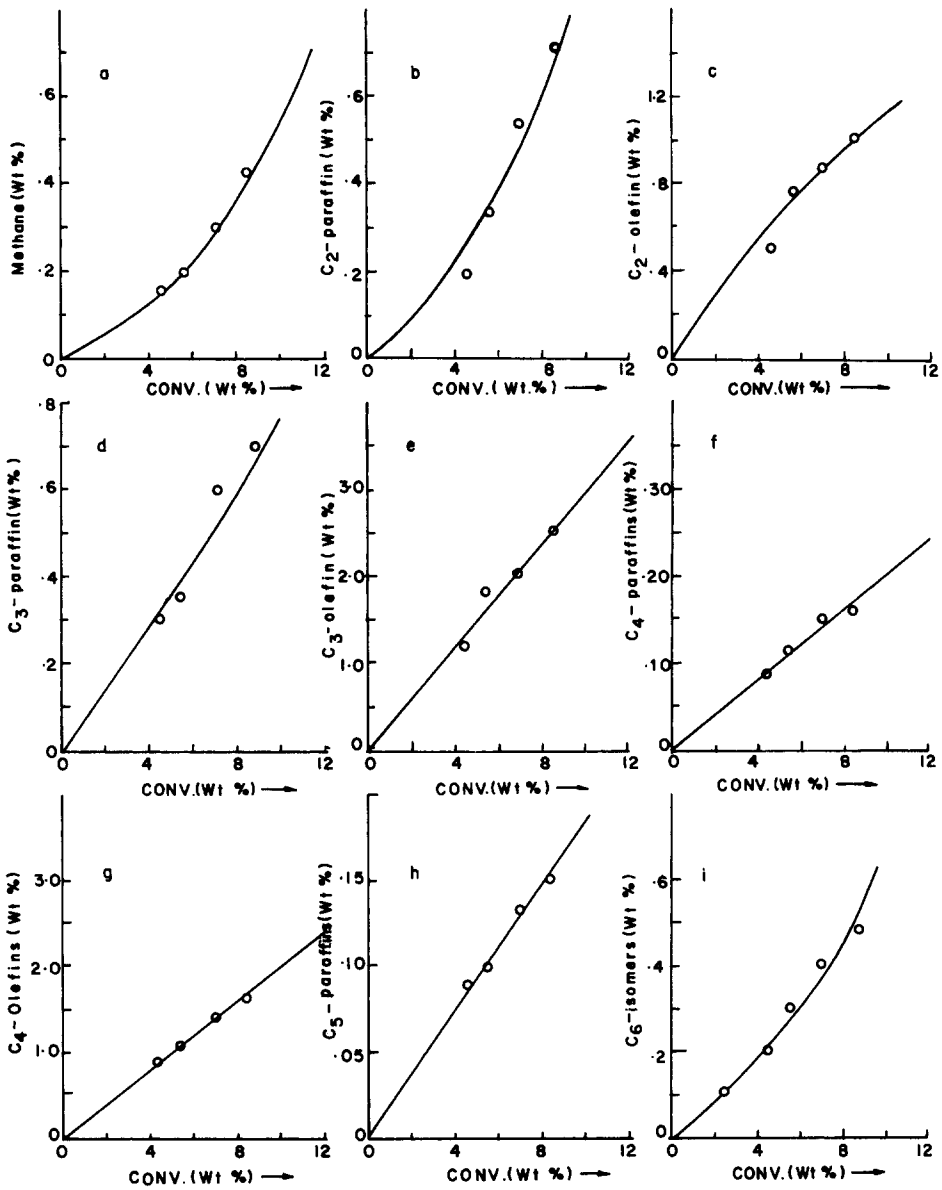

Fig. 3. Optimum performance envelopes for the products of the reaction of *n*-hexane over H-ZSM-48 at 500°C: (a) Methane; (b) C_2-paraffin C_2-olefin; (d) C_3-paraffin; (e) C_3-olefin; (f) C_4-paraffins; (g) C_4-olefins; (h) C_5-paraffins; (i) C_6-isomers.

yields the rate equation:

$$\frac{dx}{d\tau} = \frac{[A_1\{(1-x)/(1+\varepsilon x)\} + A_2\{(1-x)/(1+\varepsilon x)\}^2](1+Gt)^{-N}}{1+B\{(1-x)/(1+\varepsilon x)\}}, \qquad (1)$$

Table 1
Initial weight selectivities for cracking products from *n*-hexane over ZSM-48 in the temperature range 420–500°C

Product	Initial weight selectivities		
	420	450	500
H_2	0.0007	0.0009	0.0010
C_1	0.006	0.007	0.008
C_2-paraffin	0.059	0.080	0.083
C_2-olefin	0.101	0.125	0.146
C_3-paraffin	0.064	0.084	0.093
C_3-olefin	0.288	0.313	0.326
C_4-paraffins	0.017	0.021	0.025
C_4-olefins	0.186	0.196	0.206
C_5-paraffins	0.014	0.017	0.019
C_5-olefins	0.034	0.040	0.048
C_6-isomers	0.113	0.096	0.032
C_6-olefins	0.060	0.039	0.034
Coke	0.020	0.013	0.009
Total	0.9627	1.0315	1.0300

Table 2
Initial molar selectivities for cracking from n-hexane over ZSM-48 in the temperature range 420–500°C

Product	Initial molar selectivities		
	420	450	500
H_2	0.032	0.040	0.051
C_1	0.030	0.037	0.043
C_2-paraffin	0.200	0.229	0.237
C_2-olefin	0.310	0.383	0.448
C_3-paraffin	0.124	0.163	0.181
C_3-olefin	0.604	0.640	0.667
C_4-paraffins	0.024	0.031	0.037
C_4-olefins	0.286	0.301	0.316
C_5-paraffins	0.016	0.019	0.023
C_5-olefins	0.042	0.050	0.060
C_6-isomers	0.113	0.096	0.032
C_6-olefins	0.062	0.040	0.035
Coke	0.016	0.010	0.007
Total	1.859	2.039	2.136

where x is the instantaneous fractional conversion of the reactant, τ is the contact time, G is the deactivation rate constant, N is the decay exponent, and ε is the volume expansion coefficient. A detailed development of the Eq. (1) is described elsewhere [15].

Considering equilibrium between olefins and the corresponding carbenium ions, the constant A_1, A_2 and B are defined as [15]:

$$A_1 = \frac{(\Sigma k_{M_i})K_A + [\Sigma_i(\Sigma_j k_{c_j})_i K_i S_i]C_{A_0}}{1 + \Sigma K_i S_i C_{A_0}}[P]_0 \tag{2}$$

$$A_2 = \frac{-[\Sigma_i(\Sigma_j k_{c_j})_i K_i S_i]C_{A_0}}{1 + \Sigma K_i S_i C_{A_0}}[P]_0 \tag{3}$$

$$B = \frac{[K_A - (\Sigma_i K_i S_i)]C_{A_0}}{1 + \Sigma K_i S_i C_{A_0}} \tag{4}$$

where,

K_{M_i}	is the rate constant of a feed molecule undergoing ith mode of monomolecular protolysis,
k_{c_j}	is the rate constant of a carbenium ion $[C_jH_{2j+1}]^+$ and a feed molecule undergoing the jth mode of bimolecular chain reaction,
K_A	is the absorption constant of the feed molecule,
K_i	is the adsorption constant of the ith product,
C_{A_0}	is the initial concentration of the reactant,
$[P]_0$	is the initial concentration of the active sites,
S_i	is the molecular selectivity of the ith product.

The optimum values of the kinetic parameters A_1, A_2, B, G and N at different temperatures were determined using the nonlinear optimization technique based on Marquardt's method [16] and have been listed in Table 3. Using the optimum

Table 3
Optimum values of the kinetic parameter in the cracking of n-hexane over H-ZSM-48 in the temperature range 420–500°C

	Temperatures		
	420	450	500
Kinetic parameters			
A_1 (h^{-1})	0.17	0.30	1.98
A_2 (h^{-1})	−0.019	−0.095	−0.100
B	−0.918	−0.913	−0.901
G (h^{-1})	90.0	98.0	99.9
N	0.30	0.26	0.22
K_A/K_P [a]	0.14	0.17	0.20
K_P [b] ($l\ mol^{-1}$)	377.4	337.7	298.7
Statistical analysis			
Variance	8.5×10^{-4}	1.7×10^{-4}	1.7×10^{-4}
Standard deviation	2.9×10^{-2}	1.3×10^{-2}	1.3×10^{-2}
Correlation coefficient	0.99	0.97	0.95

[a] Determined according to Eq. (17).
[b] Determined according to Eq. (18).

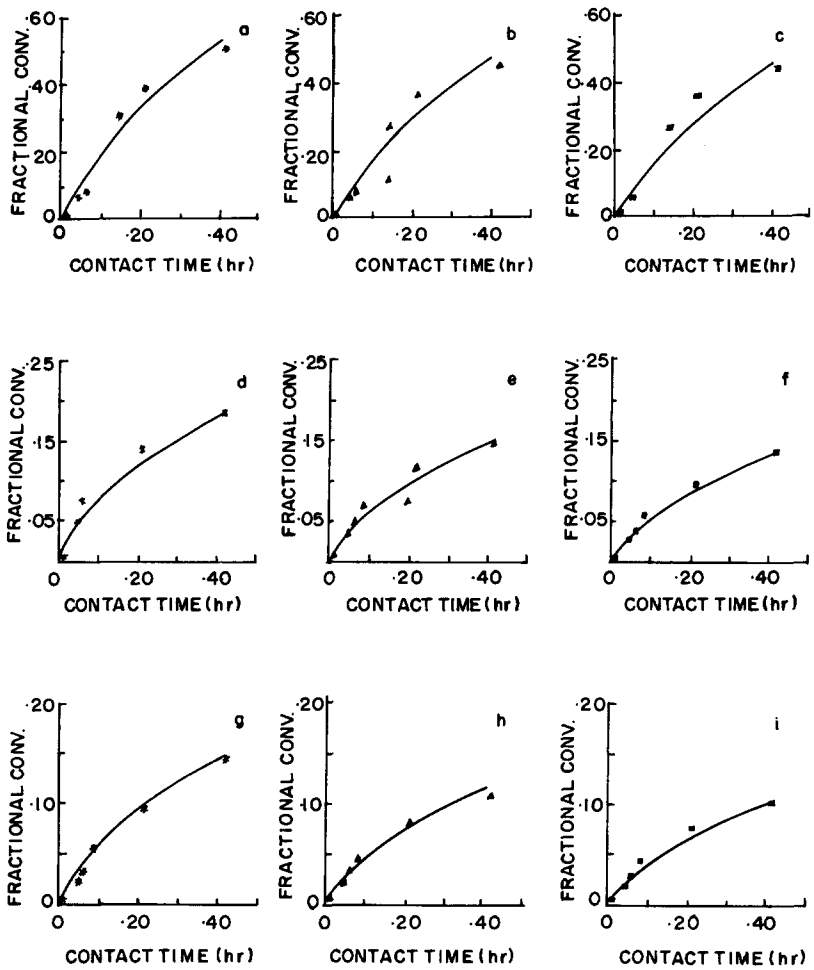

Fig. 4. Model predicted and experimental conversions as a function of contact time at different temperatures over H-ZSM-48: model predicted values (line), experimental value (points); (a–c) at 420°C (ε=0.95); (d–f) at 450°C (ε=1.00); (g–i) at 500°C (ε=1.03); time on stream =5 min (*); 15 min (▲); 30 min (■) for 420°C and 450°C; time on stream =15 min (*); 30 min (▲); and 45 min (■) for 500°C.

parameter values (Table 3) the differential Eq. (1) was integrated using the fourth order Runge–Kutta method. Fig. 4 shows the experimental and model fitted values of the fractional conversions as a function of contact time for different reaction times at three reaction temperatures. The values of standard deviation and correlation coefficient between the model fitted and the experimental conversions have been computed and presented in Table 3. The lower values of the standard deviation and the higher values of the correlation coefficients indicate that the agreement between the experimental and predicted values is satisfactory in all conditions.

2. Experimental

The feed *n*-hexane (>99%) was obtained from Merck (Bombay, India) and used without further purification. The Na-form of the zeolite was prepared from a solution containing hexamethonium bromide (used as the organic template) according to the procedure described by Valyocsik [17]. H-ZSM-48 (SiO_2/Al_2O_3=228) was obtained by three exchanges of the Na-form, with an aqueous solution of ammonium acetate (solid/solution (g/g)=1 : 10; 5N; 6 h at 353 K each exchange) and by calcination of the ammonium form at 793 K for 16 h in flowing air. The H-ZSM-48 power so obtained was pelleted, crushed and sieved to obtain 20–30 mesh particles. All the experiments were performed in a tubular down-flow glass reactor (12 mm i.d × 40 cm) with an independently controlled two-zone heater. The catalyst bed consisted of catalyst dilute by quartz chips silica of the same size (dilution=1 : 5) in order to minimize the thermal effect of the reaction. Both the liquid and gaseous samples were collected periodically and mass balances were carried out. Details of the experimental set-up and product analysis are described elsewhere [18]. Preliminary thermal cracking experiments were carried out by pumping *n*-hexane through the reactor packed with inert quartz. The experiments were performed to determine the extent of the contribution of non-catalytic cracking to the total conversion of *n*-hexane. All reaction conditions and the amount of feed were same as those used in the presence of the catalyst.

3. Results

3.1. Catalytic cracking

Data in Tables 1 and 2 show that the major initial products are C_2, C_3 and C_4 olefins, including various skeletal isomers of the feed such as: 2,2-dimethylbutane, 2,3-dimethylbutane, 2-methylpentane and 3-methylpentane. Other important initial products include C_2, C_3 paraffins and C_6^+ aliphatics. Small amounts of C_1, C_4 and C_5 paraffins were also detected in the product mixture.

3.2. Reaction mechanism

The formation of C_1–C_6 paraffins and olefins can be explained as follows: the initial process involves the protonation of *n*-hexane on a Bronsted acid site to form a $[C_6H_{15}]^+$ carbonium ion. This carbonium ion decomposes to form either hydrogen and a *n*-hexane carbenium ion $[C_6H_{13}]^+$ or into a smaller paraffin $[C_{6-n}H_{2(6-n)+2}]$ and a small carbenium ion $[C_nH_{2n+1}]^+$ (where *n* changes from 2 to 5) which replaces the proton on the Bronsted base. All the protolytic cracking steps

can be written explicity as:

$$C_6H_{14} + H^+B^- \rightarrow C_6H_{15}^+B^- \rightarrow H_2 + C_6H_{13}^+B^- \quad (5)$$

$$C_6H_{14} + H^+B^- \rightarrow C_6H_{15}^+B^- \rightarrow CH_4 + C_5H_{11}^+B^- \quad (6)$$

$$C_6H_{14} + H^+B^- \rightarrow C_6H_{15}^+B^- \rightarrow C_2H_6 + C_4H_9^+B^- \quad (7)$$

$$C_6H_{14} + H^+B^- \rightarrow C_6H_{15}^+B^- \rightarrow C_3H_8 + C_3H_7^+B^- \quad (8)$$

$$C_6H_{14} + H^+B^- \rightarrow C_6H_{15}^+B^- \rightarrow C_4H_{10} + C_2H_5^+B^- \quad (9)$$

Depending on the probabilities of the various steps, the carbenium ions in Eqs. (5)–(9) can either desorb as an olefin or participate in bimolecular chain reactions. The general form of a biomolecular reaction between a carbenium ion and a gas phase feed molecule can be written as:

$$C_6H_{14} + [C_nH_{2n+1}]^+B^- \rightarrow C_mH_{2m+2} + [C_kH_{2k+1}]^+B^- (n \neq m), \quad (10)$$

where $2 \leq n \leq 6$, $2 \leq m \leq 6$, and $2 \leq k \leq 6$.

The chain transfer process involves the rearrangement of the absorbed carbenium ions before disproportionation or desorption occurs. When such a rearrangement is followed by a hydride transfer from *n*-hexane to the rearranged carbenium ion, isomeric paraffins are produced according to the general expression:

$$C_6H_{14} + i - [C_nH_{2n+1}]^+B^- \rightarrow i - C_nH_{2n+2} + [C_6H_{13}]^+B^-. \quad (11)$$

After hydrine transfer from *n*-hexane, the carbenium ion $[C_6H_{13}]^+B^-$ is formed which undergoes a number of hydride shifts to form a variety of C_6 isomers. In the last step i.e., the chain termination step, desorption of the carbenium ion takes place as an olefin after β-scission or it remains on the surface to form coke.

4. Discussion

The results in Table 3 reveal that cracking of *n*-hexane over H-ZSM-48 proceeds predominantly via a monomolecular protolytic pathway and the probability of the protolytic cracking increases with temperature. Table 3 shows that both the parameters A_1 and A_2, increase with increasing temperature, and at all temperatures, the value of A_1 is greater than the corresponding value of A_2. It is known that in a system where chain cracking is kinetically significant, the parameter A_2 will be negative and smaller in magnitude than A_1 and A_2 which is related to the contribution of the monomolecular process to the total conversion, is found to increase with temperature. Thus, it can be concluded that the chain mechanism becomes much less significant than the protolytic process at higher temperatures.

The parameter B described by Eq. (4) signifies the relative value of the adsorption constants of the reactant and products. The B values are found to increase (more positive) with increasing temperature. The change in the magnitude

of B from −0.918 to −0.901 and a significant change in K_p values from 377.4 to 298.7 within the temperature range 420–500°C (Table 3) suggest that at lower temperature products are more strongly adsorbed on the active sites and start desorbing at higher temperatures. The same trend in B values has also been observed in *n*-nonane cracking over HY [19], whereas a reverse trend was observed during the cracking of *n*-hexadecane [20] and 2,2,4-trimethylpentane over HY in the temperature range, 300–400°C. These observations suggest that the competitive adsorption between the reactant and the products during paraffin cracking depends upon the feed and product properties and perhaps also on the catalyst characteristics.

The large consistently negative B values imply that:

$$\text{(i)}\ \Sigma K_i S_i C_{A_0} > 1, \tag{12}$$

i.e., the system is in the region of high surface coverage by the region products and

$$\text{(ii)}\ \Sigma K_i S_i > K_A, \tag{13}$$

which indicates that the products are more readily adsorbed than the reactant. Eq. (4) upon substituing from Eq. (12), gives

$$B = \frac{K_A}{\Sigma K_i S_i} - 1, \tag{14}$$

which can be further simplified as,

$$B + 1 = \frac{K_A}{\Sigma K_i S_i} \tag{15}$$

$$= \frac{K_A}{K_P \Sigma S_i}, \tag{16}$$

where $K_P = \Sigma K_i S_i / \Sigma S_i$, is the weight averaged adsorption constants for the product species. Eq. (16) can be rearranged to give:

$$K_A / K_P = (B + 1) \Sigma S_i. \tag{17}$$

Eq. (4) after substitution from Eq. (13) and simplification reduces to:

$$K_P = \frac{-B}{(1 + B) \Sigma S_i C_{A_0}}. \tag{18}$$

K_A/K_p (Eq. (17)) represents the ratio of adsorption constants for the reactant and products. The K_A/K_P (Eq. (17)) and K_P (Eq. (18)) values were calculated separately at different temperatures and are presented in Table 3. The trends shown by these values suggest that at higher temperatures the reactant competes for the adsorption sites more successfully and the surface coverage by the products decreases rapidly. The slope of the plot of log (K_A/K_P) vs. $1/T$ (Fig. 5) gives the difference in enthalpy of adsorption between the feed and the average product. The value of $\Delta H_{ads}(\Delta H_P - \Delta H_A)$ is 1.95 kcal mol^{-1} and has been calculated using

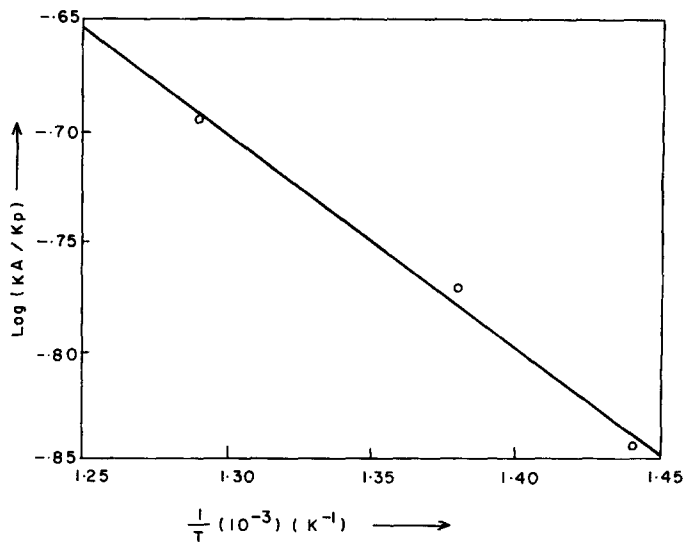

Fig. 5. Variation of log (K_A/K_P) with reaction temperature for n-hexane conversion over H-ZSM-48.

Van't Hoff relationship [21] in the temperature range 420–500°C. It is apparent that at high temperatures, under either of the two assumptions, the reactant will compete for adsorption sites more successfully.

Further insight into the rate constant is gained by adding Eqs. (2) and (3) to get,

$$A_1 + A_2 = \frac{\Sigma k_{M_i} k_A}{1 + \Sigma K_{p_i} S_i C_{A_0}} [P]_0. \tag{19}$$

By rearranging Eqs. (19) and (4), the total specific rate of monomolecular cracking can be derived as:

$$\Sigma k_{M_i} [P]_0 = \frac{A_1 + A_2}{B + 1} (1/K_A + C_{A_0}). \tag{20}$$

Substituting Eq. (12), into Eq. (20) we get,

$$\Sigma k_{M_i} [P]_0 = \frac{A_1 + A_2}{B + 1} (C_{A_0}). \tag{21}$$

Further substituting Eq. (13) into Eq. (20) results in,

$$\Sigma k_{M_i} K_A [P]_0 = \frac{A_1 + A_2}{B + 1} \tag{22}$$

The values of $\Sigma k_{M_i}[P]_0$ and $\Sigma k_{M_i} K_A [P]_0$ signifies the total specific rate of monomolecular cracking at high and low surface coverage conditions. The slopes of the plot of $\ln\{\Sigma k_{M_i}[P]_0\}$ vs. $1/T$ and $\Sigma k_{M_i} K_A [P]_0$ vs. $1/T$ give the apparent activation energies for the low and high surface coverage conditions (Fig. 6a and

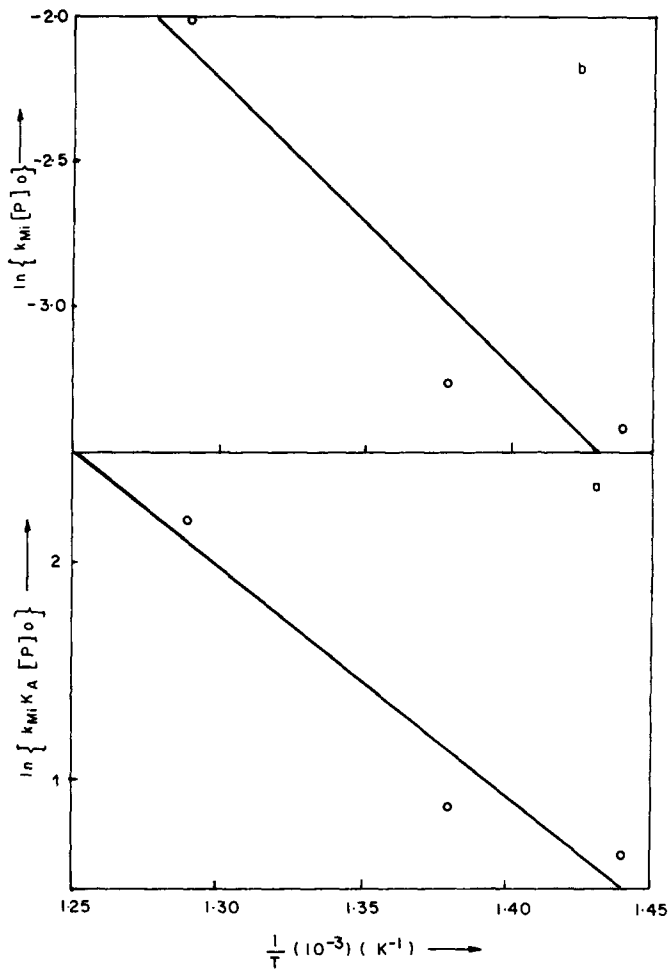

Fig. 6. Arrhenius plot for *n*-hexane protolytic cracking on H-ZSM-48 in the temperature range 420–500°C; (a) high surface coverage condition (b) low surface coverage condition.

6b). Fig. 6a and 6b show that the experimental points deviate less at higher temperature which explains the higher probability of monomolecular process at higher temperature during *n*-hexane cracking over H-ZSM-48. The E_a values for high and low surface coverage conditions are 21.0 kcal mol^{-1} and 19.3 kcal mol^{-1} respectively, which are much lower than the C–C bond dissociation energy (81 kcal mol^{-1}) [22]. A low activation energy has also been observed for cumene cracking over HY zeolite [23]. The lower activation energy for the reaction under study is probably due to the endothermic formation of the carbenium ion which exists as a metastable activated species.

The higher initial selectivities of C_4 and C_3 olefins, compared to the C_2 olefin (Table 1) can be explained by considering the formation of a bimolecular transition

state during hydride transfer from *n*-hexane to lower olefins. According to Haag et al. [24] the cross-section of the transition state complex during the hydride transfer reaction between a secondary carbenium ion and *n*-hexane is 4.8 × 6.0 Å. The sizes of the transition state complexes between *n*-hexane and a primary carbenium ion or a tert-butyl carbenium ion are 4.8 × 6.1 Å or 5.2 × 6.7 Å, respectively[1]. This implies that the reaction between *n*-hexane and the tert-butyl carbenium ion should be strongly constrained inside the pores of ZSM-48, since the cross-section of ZSM-48 is 5.3 × 5.6 Å. Lukyanov et al. [12] have showed that the hydrogenation activity of C_3 and C_4 olefins depend on the void space inside the zeolite. Among HY, H-mordenite and H-ZSM-5 showed the least activity. The comparison of our results with those obtained over H-ZSM-5 [25] at the same temperature reveals that the initial selectivities for C_4 paraffins are higher in H-ZSM-5 as compared to H-ZSM-48. This may be due to the formation of the bimolecular hydride transfer transition state complex at the channel intersection in H-ZSM-5.

5. Conclusions

In this paper a general kinetic model that includes both monomolecular protolytic cracking and bimolecular chain cracking mechanisms is shown to be applicable for a medium pore zeolite like H-ZSM-48. The ratio of the adsorption of the feed and the average product and the change in enthalpy suggest that at higher temperatures the possibility of the adsorption of the reactant is greater than that of the products. This explains the higher probability of the monomolecular processes at higher temperatures during *n*-hexane cracking over H-ZSM-48. The lower yield of C_4 paraffins compared to C_3 and C_2 paraffins is due to the strong steric inhibition to the formation of a transition state complex between *n*-hexane and a tert-butyl carbenium ion in the channels of H-ZSM-48 during the hydride transfer reaction.

Acknowledgements

DB thanks UGC, New Delhi for a senior research fellowship. We thank Prof. B.W. Wojciechowski, Queen's University, Canada for his valuable suggestions.

References

[1] P.B. Weisz and J.N. Miale, J. Catal., 4 (1965) 527.
[2] J.N. Miale, N.Y. Chen and P.B. Weisz, J. Catal., 6 (1966) 278.

[1]Size of the intermediate for *n*-hexane and primary carbonium ion, *n*-hexane and tert-butyl carbonium ion were calculated using INSIGHT II module supplied by Biosym. Inc, by a Silicon Graphics Work Station Indigo 2

[3] D.H. Olson, W.O. Haag and R.M. Lago, J. Catal., 309 (1984) 589.
[4] D.H. Olson, W.O. Haag, R.M. Lago and P.B. Weisz, Nature, 309 (1984) 589.
[5] V.J. Frillette, W.O. Haag and R.M. Lago, J. Catal., 67 (1981) 218.
[6] J. Abbot and B.W. Wojciechowski, J. Catal., 113 (1988) 353.
[7] J. Abbot, J. Catal., 126 (1990) 628.
[8] A.F.H. Wielers, M. Vaarkamp and M.F.M. Post, J. Catal., 127 (1991) 51.
[9] Y. Zaho, G.R. Bamwenda and B.W. Wojciechowski, J. Catal., 142 (1993) 465.
[10] G.R. Bamwenda, Y.X. Zhao and B.W. Wojciechwoski, J. Catal., 150 (1995) 243.
[11] Y. Zhao and B.W. Wojciechowski, J. Catal., 142 (1993) 499.
[12] D.B. Luckyanov, J. Catal., 147 (1994) 494.
[13] J. Abbot and B.W. Wojciechowski, J. Catal., 104 (1987) 80.
[14] A.N. Ko and B.W. Wojciechowski, Prog. React. Kinet., 12 (1983) 201.
[15] W.A. Gorten and B.W. Wojciechowski, J. Catal., 140 (1993) 262.
[16] D.W. Marquardt An Algorithm for Least Squares estimation of Non linear parameters, J. Soc. Ind. Appl. Math, 11 (1963) 431.
[17] E.M. Valyocsik, Eur. Patent. Appl. EPA 0142317 (1984).
[18] D. Bhattacharya, M. Chatterjee and S. Sivasankar, React. Kinet. Catal. Lett., (in press).
[19] J. Abbot and B.W. Wojeciechowski, J. Catal., 109 (1988) 274.
[20] J. Abbot and B.W. Wojeciechowski, J. Catal., 113 (1988) 353.
[21] A. Clark, The Theory of Adsorption and Catalysis, Academic Press, New York, 1970.
[22] Y. Zho, G.R. Bamwenda, W.A. Groten and B.W. Wojciechowski, J. Catal., 140 (1993) 243.
[23] D.A. Best and B.W. Wojciechowski, J. Catal., 47 (1977) 343.
[24] W.O. Haag, R.M. Lago and P.B. Weisz, Faraday Discussion., 72 (1982) 317.
[25] J. Abbot, Appl. Catal., 57 (1990) 105.